

## AlGaN-based ultraviolet light-emitting diodes grown on AlN epilayers

K. H. Kim, Z. Y. Fan, M. Khizar, M. L. Nakarmi, J. Y. Lin, and H. X. Jiang<sup>a)</sup>

*Department of Physics, Kansas State University, Manhattan, Kansas 66506-2601*

(Received 8 June 2004; accepted 28 September 2004)

AlGaN-based deep-ultraviolet light-emitting diode (LED) structures, which radiate light at 305 and 290 nm, have been grown on sapphire substrates using an AlN epilayer template. The fabricated devices have a circular geometry to enhance current spreading and light extraction. Circular UV LEDs of different sizes have been characterized. It was found that smaller disk LEDs had higher saturation optical power densities but lower optical powers than the larger devices. This trade-off between power and power density is a result of a compromise between electrical and thermal resistance, as well as the current crowding effect (which is due to the low electrical conductivity of high aluminum composition *n*- and *p*-AlGaN layers). Disk UV LEDs should thus have a moderate size to best utilize both total optical power and power density. For 0.85 mm × 0.85 mm interdigitated LEDs, a saturation optical power of 2.9 mW (1.8 mW) at 305 nm (290 nm) was also obtained under dc operation. © 2004 American Institute of Physics. [DOI: 10.1063/1.1819506]

In recent years, there has been a great effort to develop AlGaN-based compact ultraviolet light-emitting diodes (LEDs) with a wavelength ( $\lambda$ ) below 360 nm for applications such as solid-state lighting and biochemical agent detection. For deep-UV emission with  $\lambda < 340$  nm, the quantum-well (QW) structure based LED requires an active layer with Al composition higher than 20%. Inevitably, the alloy composition for the *p* and *n* cladding should be more than that of the active layer. The high Al composition introduces not only dislocations, but also leads to poor *p*- and *n*-type conductivity in the cladding layers, which limits current injection.<sup>1</sup> Achieving *p*-AlGaN with high Al composition by Mg doping is a challenging issue. Different material structures have been utilized to improve the material quality and the UV LED power level.<sup>1-8</sup> Concerns have arisen because of current crowding and inhomogeneous driving in the standard 300  $\mu\text{m}$  × 300  $\mu\text{m}$  square geometry lateral LEDs.<sup>9</sup> The lateral structure and the poor conductivity of the *n* and *p* cladding layers lead to current crowding and the inhomogeneous effect,<sup>10</sup> which can significantly limit the output optical power density.

In this letter, we report on the fabrication and characterization of deep-UV LEDs grown on sapphire substrate using an AlN epilayer template. The benefits of inserting an AlN epitaxial layer as a template for the growth of subsequent III-nitride device structures have been demonstrated in several experiments.<sup>11,12</sup> It was previously shown that GaN epilayers grown on AlN/sapphire templates comprise a lower dislocation density compared with the GaN grown directly on sapphire using low-temperature GaN buffer.<sup>11</sup> It was recently demonstrated that InGaN LEDs grown on the AlN/sapphire template exhibited a higher output power and a better thermal stability compared to the conventional LED grown on sapphire using a low-temperature GaN buffer layer. This is due to the reduced threading dislocation density in the active layer and higher thermal conductivity of the AlN epilayer.<sup>12</sup>

Recently, our group has established growth conditions for achieving high quality AlN epilayers on sapphires by metalorganic chemical vapor deposition (MOCVD).<sup>13</sup> Be-

cause of the known benefits of using AlN epilayer as a template for nitride devices and its excellent UV transparency down to 200 nm, the insertion of AlN epilayer as a template for UV LED structures becomes a natural choice. By using an AlN epilayer as the template for the growth of the *n*-AlGaN layer, it was found that the overall quality, including crystalline quality, surface morphology, photoluminescence (PL) intensity, and the conductivity of the *n*-AlGaN epilayer exhibited a remarkable improvement compared to *n*-AlGaN epilayers grown directly on the low-temperature AlN buffer layer.<sup>14</sup> The high quality AlN epilayer acted as a dislocation filter for the growth of subsequent device layers.<sup>11,12</sup>

The UV LED structure was deposited on the basal plane sapphire substrate by MOCVD. A high quality AlN epilayer with a thickness of about 1  $\mu\text{m}$  was grown as the epitaxial template for the subsequent device layers. On the AlN epilayer, a 1.5  $\mu\text{m}$  Si-doped *n*-Al<sub>0.6</sub>Ga<sub>0.4</sub>N was grown as the *n*-type contact layer. Following is the active region consisting of a three-period Al<sub>0.35</sub>Ga<sub>0.65</sub>N (2.5 nm)/Al<sub>0.4</sub>Ga<sub>0.6</sub>N (3.0 nm) or Al<sub>0.4</sub>Ga<sub>0.6</sub>N (2.5 nm)/Al<sub>0.5</sub>Ga<sub>0.5</sub>N (3.0 nm) multiple QWs for 305 or 290 nm LEDs. Since it is difficult to achieve a reasonable hole density in an AlGaN alloy with high Al composition, a *p*-Al<sub>0.7</sub>Ga<sub>0.3</sub>N layer (10 nm) was employed as an electron blocking layer to effectively block the electron overflow, thereby enhance the electron-hole radiative combination in the QWs. The use of this electron blocking layer has been previously demonstrated in UV LEDs by several groups.<sup>5-8</sup> The structure was then completed with a 60 Å Mg-doped *p*-Al<sub>0.6</sub>Ga<sub>0.4</sub>N and 150 nm heavily doped *p*-Al<sub>0.1</sub>Ga<sub>0.9</sub>N as the *p* contact layer. In the circular LED, the *p* contact is in the middle and the *n* contact encircles the mesa disk. The fabrication started from the deposition of Ni/Au transparent layer and the mesa etching to expose the *n*-Al<sub>0.6</sub>Ga<sub>0.4</sub>N, followed by Ti/Al metal deposition for the *n* contact and Ni/Au for *p* contact with rapid thermal annealing at 650 °C for 2 min. LEDs with different mesa disk sizes were then diced into single devices, flip-chip bonded with Au bumps onto ceramic AlN submount, and finally mounted on TO headers. A calibrated UV integrating optical sphere was used to measure the light output power from the sapphire

<sup>a)</sup>Electronic mail: jiang@phys.ksu.edu

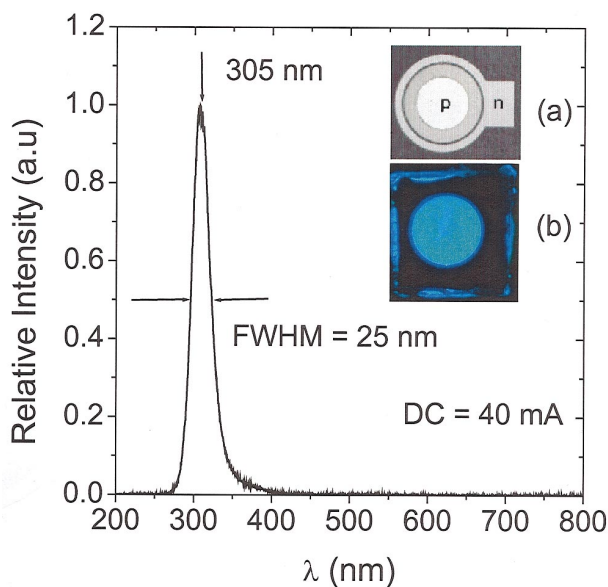


FIG. 1. (Color) EL spectrum of a 305 nm UV LED under 40 mA dc driving current. The inset shows the optical microscope images of (a) the fabricated LEDs with circular geometry, and (b) light emission from sapphire side of the flip-chip bonded LED.

side since the submount side is nontransparent. Compared with the usual square geometry, circular geometry with  $n$  contact encircles the  $p$ -type mesa disk is an option to overcome the current crowding phenomenon. Circular LEDs with different disk sizes were fabricated to study the size dependence.

The electroluminescence (EL) spectrum of a representative LED under 40 mA dc driving is shown in Fig. 1, along with microscope images of the fabricated circular LED geometry and sapphire-side light emission from the flip-chip bonded LED. The emission has a 305 nm peak with a full width at half-maximum of 25 nm. The intensity of the often-observed long-wavelength emission from 350 to 400 nm has been dramatically reduced. During the structure optimization, each layer was etched off sequentially and then PL measurements were taken. It was found that the long-wavelength emission is caused mainly by electron recombination in the  $p$  cladding layer with deep-level impurities<sup>8,15</sup> associated most likely with cation vacancies.<sup>14,16</sup> By incorporating an electron blocking layer, the injected electrons can be more effectively confined in the active region, diminishing the long-wavelength emission. Another observed contribution to the pure emission spectrum comes from the high quality AlN template and the subsequent low defect structure, especially reduction of other recombination channels in the  $n$  cladding layer.

The mesa disk size (diameter  $d$ ) can influence the UV LED performance, including the turn-on voltage, differential resistance, output power, and power density, etc. The  $I$ - $V$  characteristics of LEDs with different disk sizes for 305 nm LEDs are compared in Fig. 2, and the inset lists forward voltage  $V_F$  at 20 mA. As the disk diameter  $d$  increases from 85 to 310  $\mu\text{m}$ ,  $V_F$  decreases from 13.4 to 12.0 V as a result of larger area and lower series resistance. Both the  $V_F$  values and the turn-on voltages ( $>8$  V) are relatively high, which is a result of the use of relatively high aluminum concentration (60%) in the  $n$  and  $p$  cladding layers and consequently lower quality  $n$  and  $p$  ohmic contacts. Figure 3

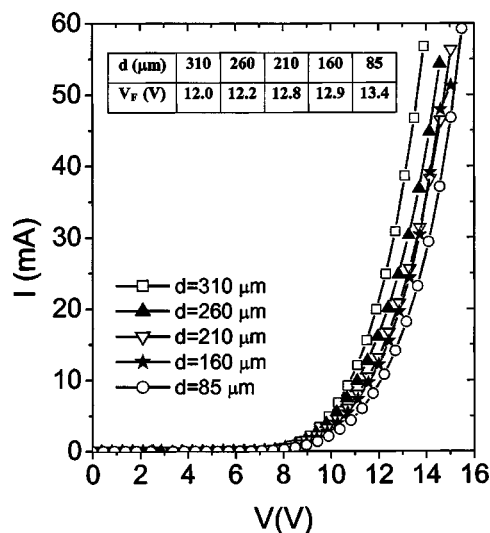


FIG. 2.  $I$ - $V$  characteristics of the circular 305 nm UV LEDs with different mesa disk diameters  $d$ . The inset lists the forward voltage  $V_F$  at 20 mA.

compares the dc characteristics of optical output power versus current ( $L$ - $I$ ) and power density versus current of 305 nm LEDs. In general, it can be derived from Fig. 3(a) that at a low driving current ( $<20$  mA), the light output is similar, with no significant dependence on the disk size. With increased input current, the thermal effect becomes important and the light output gradually saturates. Under the same driving current, the smaller disk with a smaller bonding area to the submount has a larger thermal resistance and a larger thermal intensity; therefore, it has a lower saturation optical power output. On the other hand, when the disk size is larger than 210  $\mu\text{m}$ , the output power again becomes almost independent of the disk size, which is attributed to the current crowding phenomenon. At a high level of current driving, the large resistance of the  $n$ -Al<sub>0.6</sub>Ga<sub>0.4</sub> layer causes the current distribution to become more and more inhomogeneous and

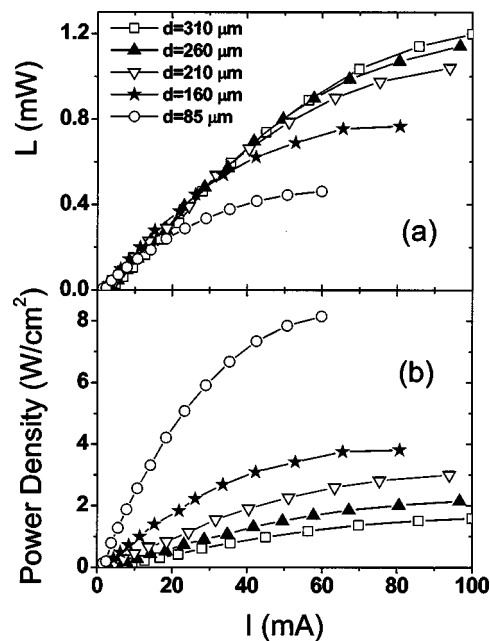


FIG. 3. (a) Optical power output vs current and (b) optical power density vs current of the circular 305 nm UV LEDs with different mesa disk diameters under dc driving, measured in a calibrated UV integrated optical sphere.

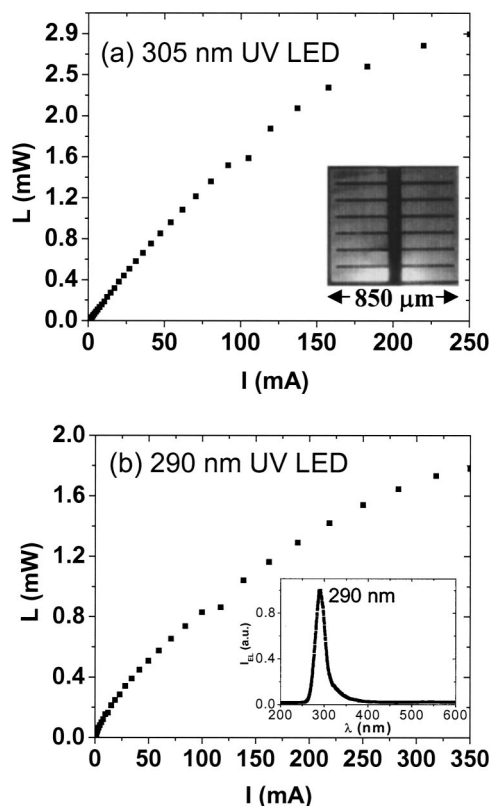


FIG. 4. Optical output power vs current characteristics of  $0.85 \text{ mm} \times 0.85 \text{ mm}$  interdigitated UV LEDs under a dc driving for (a) 305 nm and (b) 290 nm devices, measured in a calibrated UV integrated optical sphere. The inset in (a) shows the optical microscope image of a fabricated interdigitated UV LED and (b) shows the EL spectrum of a 290 nm UV LED.

more concentrated on the disk edge region, so that the maximum output power increases only slightly with the disk size.

Figure 3(b) shows that under the same current driving (before saturation), the output power density of the smaller disk is much higher than that of a larger disk. Specifically, the  $85 \mu\text{m}$  disk LED has a saturation optical power density of  $8.0 \text{ W/cm}^2$  and power of  $0.46 \text{ mW}$  at  $60 \text{ mA}$ . The  $310 \mu\text{m}$  disk LED has a saturation optical power density of  $1.6 \text{ W/cm}^2$  and power of  $1.2 \text{ mW}$  at  $100 \text{ mA}$ . With a trade-off between the total output power and the power density, the optimized LED disk should have a moderate size of  $\sim 250 \mu\text{m}$ . As the material quality further improves, especially the conductivity of  $n$  and  $p$  cladding layers, we believe that the optimized disk size would also be larger, which should further enhance the total optical power output.

Since the current spreading problem puts a limitation on the disk size, to further increase the total output power by increasing the light emission area, the  $n$  contact should be introduced into the mesa area to keep the mesa dimension in the limitation of current spreading distance. An interconnected-disk LED is an option.<sup>4</sup> Here, we also employ the more common interdigitated device geometry to achieve higher optical output power. The fabricated  $0.85 \text{ mm} \times 0.85 \text{ mm}$  LEDs have an emission area of  $0.72 \text{ mm}^2$ . As shown in Fig. 4, we have achieved saturation optical powers of  $2.9$  and  $1.8 \text{ mW}$  for the  $305 \text{ nm}$  and  $290 \text{ nm}$  UV LEDs, respectively, under a dc driving.

For applications such as biochemical agent detection, the total optical output power and optical power density are critical specifications. Small-aperture (disk size) UV light emitters, which possess a much higher power density, could be a

better choice than the large ones. As previously discussed, the limitation of the small-disk LED to achieve a higher power results from a larger thermal resistance, caused by the small size of Au bumps under the  $n$  and  $p$  contacts. For a given disk size, although the maximum  $p$  contact and the related Au bump size have been determined, there is no limitation on  $n$  contact and the underneath bump size. With an enlarged  $n$  contact and the bump, thermal dissipation of the small-disk LED should be improved to achieve a higher output optical power.

In summary, AlGaIn-based 305 and 290 nm UV-LEDs structures have been grown on sapphire substrates using AlN epilayer templates. The performance of LEDs with different disk sizes is compared. The high performance disk LED has a moderate size of  $\sim 250 \mu\text{m}$  due to a trade-off between the maximum optical power and power density (which is necessary because of the thermal effect and the current crowding problem). The high resistivity of  $n$  and  $p$  cladding layers not only increases  $V_F$ , but also causes the current spreading problem for the lateral structure LED. For flip-chip bonded devices, the  $p$  metal contact may be designed to have a similar size as the mesa ( $p$ - $n$  junction area) to eliminate the influence of the highly resistant  $p$  cladding layer on current spreading. To relieve the influence of the  $n$  cladding layer on large-sized devices and to increase the total optical output power, the  $n$  contact should be introduced into the mesa area to keep the mesa dimension in the limitation of current spreading distance. Based on our results, we believe that high quality AlN epilayers will be particularly important and useful as a template for the growth of UV emitters operating below  $300 \text{ nm}$ .

This work is supported by the grants from DARPA, ARO, NSF, and DOE.

- <sup>1</sup>T. Nishida, H. Saito, and N. Kobayashi, Appl. Phys. Lett. **78**, 399 (2001).
- <sup>2</sup>H. Hirayama, Y. Enomoto, A. Kinoshita, A. Hirata, and Y. Aoyagi, Phys. Status Solidi A **180**, 157 (2000).
- <sup>3</sup>A. Chitnis, J. P. Zhang, V. Adivarahan, M. Shatalov, S. Wu, R. Pachipulusu, V. Mandavilli, and M. Asif Khan, Appl. Phys. Lett. **82**, 2565 (2003).
- <sup>4</sup>K. H. Kim, J. Li, S. X. Jin, J. Y. Lin, and H. X. Jiang, Appl. Phys. Lett. **83**, 566 (2003).
- <sup>5</sup>A. Yasan, R. McClintock, K. Mayes, D. Shiell, L. Gautero, S. R. Darvish, P. Kung, and M. Razeghi, Appl. Phys. Lett. **83**, 4701 (2003).
- <sup>6</sup>A. J. Fischer, A. A. Allerman, M. H. Crawford, K. H. A. Bogart, S. R. Lee, R. J. Kaplar, W. W. Chow, S. R. Kurtz, K. W. Fuller, and J. J. Figiel, Appl. Phys. Lett. **84**, 3394 (2004).
- <sup>7</sup>V. Adivarahan, S. Wu, J. P. Zhang, A. Chitnis, M. Shatalov, V. Mandavilli, R. Gaska, and M. Asif Khan, Appl. Phys. Lett. **84**, 4762 (2004).
- <sup>8</sup>A. Hanlon, P. M. Pattison, J. F. Kaeding, R. Sharma, P. Fini, and S. Nakamura, Jpn. J. Appl. Phys., Part 2 **42**, L628 (2003).
- <sup>9</sup>M. Shatalov, G. Simin, V. Adivarahan, A. Chitnis, S. Wu, R. Pachipulusu, V. Mandavilli, K. Simin, J. P. Zhang, J. W. Yang, and M. A. Khan, Jpn. J. Appl. Phys., Part 1 **41**, 5083 (2002).
- <sup>10</sup>M. Iwaya, S. Takanami, A. Miyazaki, Y. Watanabe, S. Kamiyama, H. Amano, and I. Akasaki, Jpn. J. Appl. Phys., Part 1 **42**, 400 (2003).
- <sup>11</sup>S. Arulkumaran, M. Sakai, T. Egawa, H. Ishikawa, and T. Jimbo, T. Shibata, K. Asai, S. Sumiya, Y. Kuraoka, M. Tanaka, and O. Oda, Appl. Phys. Lett. **81**, 1131 (2002).
- <sup>12</sup>B. Zhang, T. Egawa, H. Ishikawa, Y. Liu, and T. Jimbo, J. Appl. Phys. **95**, 3170 (2004).
- <sup>13</sup>J. Li, B. Nam, M. L. Nakarmi, J. Y. Lin, and H. X. Jiang, Appl. Phys. Lett. **81**, 3365 (2002).
- <sup>14</sup>M. L. Nakarmi, K. H. Kim, K. Zhu, J. Y. Lin, and H. X. Jiang, Appl. Phys. Lett. (in press).
- <sup>15</sup>M. Shatalov, A. Chitnis, V. Mandavilli, R. Pachipulusu, J. P. Zhang, V. Adivarahan, S. Wu, G. Simin, M. A. Khan, G. Tamulaitis, A. Sereika, I. Yilmaz, M. S. Shur, and R. Gaska, Appl. Phys. Lett. **82**, 167 (2003).
- <sup>16</sup>C. G. Van de Walle and J. Neugebauer, J. Appl. Phys. **95**, 3851 (2004).